Research Article

Measurement of Transport Number of Lithium in Glycerol Assisted by Fourier Transform Spectroscopy Analysis: Progress towards Elaboration of Optimal Electrolyte of Friendly Environmental Battery

Fatima Moulay
Department of Electronics, Faculty of Electrical Engineering, University of Sciences and Technology of Oran - Mohamed Boudiaf (USTO-MB), Oran, Algeria

Mostefa Kameche*, Fatima Lahmar, M'hamed Mehouen, Lahouaria Annag and Hamida Nouria Baba Ahmed
Department of Chemistry, Faculty of Chemistry (LPCMCE), University of Sciences and Technology of Oran - Mohamed Boudiaf (USTO-MB), Oran, Algeria

* Corresponding author. E-mail: mostefa.kameche@univ-usto.dz DOI: 10.14416/j.asep.2021.10.001
Received: 12 April 2021; Revised: 25 May 2021; Accepted: 2 August 2021; Published online: 7 October 2021

Abstract
Up to now, a great deal of research investigations on lithium ion conductors has been carried out because they are potentially utilized in the solid electrolytes of the batteries and the electrochemical devices. However, in order to elaborate on new ecological batteries of lithium, it becomes primordial to study and understand the properties of transport of the lithium electrolytes using eco-friendly solvents to find the best electrolyte for such devices. In fact, the electromotive forces (EMFs) of lithium chloride electrolyte in the hydrogen-bonded solvents glycerol were measured using the concentration cells (CCs) 0.005/0.05 and 0.05/0.5. Then, the transport numbers of the lithium-ion were deduced by means of the Nernst equation in combination with the Debye-Huckel limiting law. Whilst, the activation energy values were calculated from the parameters of the fitting of the transference number data to the empirical power law, yielding a regression coefficient of 95.9% for the most concentrated concentration cell. The structure and interactions in the lithium electrolyte solution were studied by vibrational Infra-Red spectroscopy. The experimental data were discussed and compared to those previously obtained, using impedance spectroscopy of glass-forming glycerolate lithium electrolytes for the same purpose. Despite the enormous difference between their viscosities, glycerol shows similar activation energy (i.e., 31.40 $kJ.mol^{-1}$) with water (i.e., 31.73 $kJ.mol^{-1}$), particularly at very low concentration, confirming both solvents being hydrogen-bonded. Besides, this study suggests the utilization of the glycerol-lithium ion electrolyte for the future conception of an ecological lithium-ion battery, rather than those using ion electrolyte polymer currently on the market. Similarly to relaxation and conductivity, the transport number data suggests that the diffusion of conformational states also monitors the overall lithium-ion transport mechanism.

Keywords: Lithium, Hydrogen-bonded glycerol, Transport number, Activation energy, FTIR spectroscopy

1 Introduction

Nowadays, there is a great advance in elaborating the solid-state polymer electrolytes, which are destined to the lithium batteries of higher energy densities [1], [2]. The basic function of the electrolyte is its stability to conduct the ions. This can be achieved by determining the electric conductivity of the electrolyte and the transport number of the moving ion, i.e., the lithium-ion.

Having a high energy density, the metal lithium is largely utilized in the elaboration of the electrolytes of the lithium-ion batteries for functioning the portable electronic devices and the measuring apparatuses [3]–[5]. Owing to its importance, the transport of lithium in nonaqueous polyelectrolyte solutions has been recently investigated by molecular dynamics simulations to simulate the optimal conducting electrolyte that allows higher energy performance of the lithium battery [6].

When an electrochemical cell generates a higher current density, its performance reduces significantly. Therefore, the displacement of the lithium ion inside the electrolyte becomes a serious problem. Actually, in order to study the long lifetime lithium battery, a recent investigation in the topic has been carried out by using the ionic liquids to enchance the electrolyte/electrode interface [7]. Thus, the assessment of the transport number of the metal ion along with the electric conductivity of the electrolyte is primordial in designing lithium-based batteries [8]. Besides, the salt dissociates into lithium cation (Li^+) and halide anion (X^-: Cl^-, BF_4^-, PF_6^-…) in the electrolyte utilized in a lithium-ion battery. The two opposite species both carry the electric current densities I+ and I– respectively. The amount of each current density for the overall current density defines the transport number, namely t_{Li+}, which should be as high as possible and should consequently decrease the concentration change while the battery is in the charging or discharging processes. Unfortunately, the transport numbers of lithium in electrolyte systems such as (Li^+X^-/organic solvent) are in general less than 0.5 [9], [10].

The principal role of an electrolyte is to determine the fasting delivery of the energy stored in both electrodes of the battery [11]. It is well known that the ion in the solution is transported while surrounded by solvent molecules. Its ionic conductivity and mobility are the overall results of its solvation. Therefore, the elaboration of the conductive lithium electrolyte and the knowledge of its solvation is necessary. This latter can be determined indirectly by measuring the coordination number [12]. Amongst these methods, one may cite Ab initio calculations [13], mass spectrometry, NMR measurements [14], [15] and XRD experiments [16], [17]. The Small Angle Neutron Scattering (SANS) is well known as a powerful analytical technique for the investigation of the properties of the electrolytes and polyelectrolytes, in particular for monitoring and understanding the kinetic processes in the Li-ion batteries [18]. SANS was utilized to study the pore filling in the carbon-supported electrodes and to understand the different mechanisms limiting the lithium-air battery capacity [19].

In both primary and secondary lithium batteries, the electrolytes utilized are often mixtures of a lithium salt (solute) and organic aprotic solvents. In such electrochemical systems, the reaction of the solvent is avoided, especially in the presence of an inert atmosphere. Moreover, it is suggested in these special electrolytes the use of high dielectric solvents in order to dissolve the lithium salt sufficiently. A mixture of the two organic solvents is generally recommended for better transport properties of the electrolytes [20].

The improvement of the performance of the lithium-battery resides in the elaboration of its stable electrolyte able to efficiently transport the lithium-ion by using different temperatures. So, owing to their stable physico-chemical properties at room temperature, the polymer electrolytes are suitable materials for this purpose. Glycerol is an interesting candidate because it is thermally stable and able to coordinate lithium ions, allowing and thus increasing the formation of lithium alkoxide functionalities within the molecule. In a liquid state, it is considered for its interesting relaxation properties [21]. Moreover, the transesterification mechanism of the triacylglycerol in biodiesel production is essential to know. The molecular modeling can therefore be used to determine the geometrical parameters of triacylglycerol via Ab initio with the GaussView and Gaussian softwares. The modeling results showed the geometrical parameters of the triacylglycerol molecules and, as a result, the simulated transesterification mechanism [22].

This work reports the measurement of the transference number of the lithium ion in the high

viscous hydrogen bonded glycerol, for using afterwards as a suitable electrolyte in a less-polluted lithium battery. The concentration cell method was utilized to determine the transport number using different concentrations and temperatures. The data were then fitted to the empirical power law [23] in a temperature range and discussed in terms of the ionic transport properties of the electrolyte and the activation energy. Furthermore, FTIR spectroscopy was used to understand the structure and interactions that characterize the lithium electrolyte versus the concentration of salt.

2 Theoretical Background

The electric conductivity, the transport number, the diffusion coefficient, the ionic mobility, and the viscosity of an electrolytic solution determine the performance of a battery in general and a lithium-ion cell in particular. The knowledge of the transport of the current by the ionic species in the electrolyte is indeed primordial. It is thus important, in particular, when the higher electric currents are applied to charge or discharge a given battery. In effect, during the discharge of the battery, the Li^+ ions are taken out from the anode (negative electrode) and inserted into the cathode (positive electrode). Thus, a percentage of the current is transported by the Li^+ cations, and another percentage is by the anions moving in the opposite direction. These quantities are called transport numbers of the involved ionic species, namely t_+, and t_-, respectively. In general, the value of t_{Li+} is less than 0.5 and that of the anion greater than 0.5. This means that the non-coordinating anion (A^-) is moving more freely and carries more current than the cation. While the metal cation (Li^+) is relatively tightly bound to the solvent molecule, moving slowly and consequently transports less current.

When two electrolytic solutions of different concentrations are brought into contact in a concentration cell with the transfer of matter, the ions displacements occur across the junction. If the transfers of the cations and those of the anions differ from each other, a charge segregation is well developed at the separating liquid junction, and consequently, an electrical potential difference is produced. The latter tends to delay the more mobile ion and speed up the less mobile ion. Thus, when the velocities of the transfer of the two ions are equalized, the potential difference attains a steady value, called the potential of the liquid junction (E_{LJ}) [24]. The value of the electromotive force can be calculated using the Nernst equation [25].

As a fraction of the current is taking place in the motion of the lithium ions, the complementary fraction consists of the consumption of the lithium ions at the interface with the positive electrode (or production at the negative) quicker than the electrical migration reconstitutes it. This behavior induces, in consequence, a gradient of the concentration of the electrolyte between the electrodes. It consequently results in the gradient in the electrolyte concentration, which unfortunately limits the discharge (or charge) of the battery. If lithium salt concentration at the electrode surface vanishes, the ionic conductance becomes very low, and thus the lithium-ion battery stops to function. In contrast, if electrolyte concentration increases very much, the salt can precipitate, and the conductance again becomes very low. It may be concluded that the values of transport number of the metal cation (in our case Li^+), and the salt diffusion coefficient, determine the rapid formation of the concentration gradient, and in turn, the maximum current that the electrolyte can sustain indefinitely. Both of these parameters are, therefore, important properties of any electrolyte used in a lithium-ion battery. The electromotive force of the concentration cell with liquid junction (E_{LJ}) may be given by the Nernst equation [25]. It was thus utilized to determine the transport number (t_+) of the cation (in our case, the lithium ion).

$$t_+ = \frac{E_{LJ}\, F}{2\, RT\, Ln\left(\frac{\gamma_1 C_1}{\gamma_2 C_2}\right)} \quad (1)$$

where γ_i is the ion activity, R is the gas constant, F Faraday constant, and T is the temperature. The values of the ion activities are calculated by using the Debye-Huckel limiting law Equation (2) [26].

$$Ln(\gamma) = -\frac{e^3 \left(2N_0 C\right)^{1/2}}{8\pi\left(\varepsilon_0 \varepsilon_r KT\right)^{3/2}} \quad (2)$$

Besides, based on this law, the transference number at infinite dilution can be calculated using Equation (3) [27],

$$t^0_{Li+} = t_{Li+} \frac{\left(0.5 - t_{Li+}\right)\beta\sqrt{C}}{\Lambda^0\left(1+\kappa a\right)} \quad (3)$$

Where "β" is the electrophoretic term for the univalent electrolyte (Ω^{-1} cm^2 $mol^{-3/2}$ $L^{1/2}$) [Equation (4)] [27].

$$\beta = \frac{82.46}{\eta\left(\varepsilon_r T\right)^{1/2}} \quad (4)$$

"κ" is the inverse radius of the ionic atmosphere around a reference ion [Equation (5)] [27], [28].

$$\kappa = \left(\frac{2N_0 e^2}{\left(KT\varepsilon_0\varepsilon_r\right)^{1/2}}\right)^{1/2} \quad (5)$$

"a" is the closest approach of a distance of two univalent ions of opposite signs (called Bjerrum distance) [Equation (6)] [27], [28]

$$a = \frac{e^2}{8\pi KT\varepsilon_0\varepsilon_r} \quad (6)$$

3 Materials and Methods

3.1 *Materials*

The solute lithium chloride salt (99.99% pure) and the solvent glycerol (99.5 +% pure) were purchased from Aldrich. They were used in the experiments after further treatment. The reagents were thus dried in an oven to remove traces of water and moisture. The solutions were prepared and then stirred for 24 or 48 h before the use in the experiment. On the other hand, the silver chloride electrodes were prepared by electrolysis, according to the instructions listed elsewhere [29]–[31]. The main operating conditions were the current density of 0.2 mA/cm^2 and the electrolysis duration of 1 h. The pair of two identical electrodes, Ag/AgCl yielding a difference potential less than 0.05 mV in magnitude, was utilized in all the experiments.

3.2 *Cell set up for the measurement of the liquid junction potential*

The liquid junction cell used to measure the transference number of the moving ions consisted of two half-cells in which two reversible silver chloride electrodes were immersed in solutions with different concentrations. They can be linked to each other through a small glass tap placed at the bottom of the cell, which allows the separation between them. The cell was then placed inside another greater double envelope glass cell linked to a water bath (cryostat) by using a plastic pipe, in which the temperature was kept approximately unchanged (Figure 1). Finally, the junction between the lithium solutions was formed by gently opening the glass tap. The temperatures varied from 0 to 30°C in a step of 5°C. The desired temperature was in general, reached after one hour. The value of the electromotive force was taken from the voltmeter mounted in parallel until it was stable over a duration of 30 min.

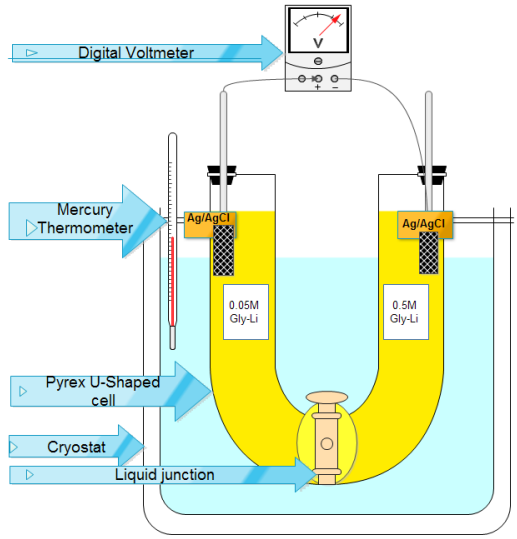

Figure 1: Experiment set up for measurement of liquid junction potential using concentration cell.

4 Results

4.1 *Transport number data*

With the concentration cell technique, the transference number of the cation metal (t_{M+}) is easily calculated by taking the ratio between the two measured electromotive forces: the electromotive force with transference (E_{LJ}) and the electromotive force without transference (with the amalgam electrodes) [32]–[34]. However, the latter was not reliable enough with the reactive lithium metal and gave incorrect values of the electromotive force. For that reason, the transport number was deduced by means of the Nernst equation Equation (1) in combination with the Debye-Huckel limiting law Equation (2).

In addition, Equations (3) and (4) were utilized to yield at the temperature 25°C, the transport number values 0.084 and 0.228 for the concentration cells 0.005/0.05 and 0.05/0.5 (mol. L^{-1}) respectively. In comparison to those obtained previously using the cation metals in glycerol, i.e., sodium (0.417) and potassium (0.479) [26], these values are relatively smaller. They are in order $t_{Li+} < t_{Na+} < t_{K+}$, which is in correlation with the standard enthalpies of hydration summarized in [34] i.e. ΔH^0_{hyd} (K^+) < ΔH^0_{hyd} (Na^+) < ΔH^0_{hyd} (Li^+). We may thus attribute this difference to the crystallographic and solvated ionic radii of the ionic species being considered.

Besides, the transference numbers of the lithium ion using the concentration cell 0.005/0.05 is 0.084, remarkably less than that of the concentration cell 0.05/0.5 (i.e., 0.228). We may attribute this large difference to the non reliability of Equation (1) in calculating the transference number from the very dilute concentration cell displaying an electric resistance greater than 1 MΩ. An alternative electrochemical method should be implemented experimentally to find the reliable data at the lowest concentrations.

As shown in Table 1, the values at infinite dilute dilution (i.e. C → 0) are calculated with the Debye-Huckel limiting law using the two nominal concentrations 0.05 and 0.5 mol/L of the most reliable concentration cell. The values obtained are 0.245 and 0.283, respectively, allowing an increase of 15%. However, if we take the previous values of sodium and potassium in glycerol [26], we find just an increase of 2% and less than 1%, respectively, which permits us to say that the transport number of lithium is very much sensitive to the variation of concentration since it is a very reactive metal. The calculated values are grouped in Table 1 and other solvents displaying the hydrogen bonds (i.e., water, ethylene glycol, ethanol, and methanol). The data given above are consistent with the classification of the solvents according to the number of their hydroxyl groups: with one hydroxyl group (ethanol and methanol), with two hydroxyl groups (water and ethylene glycol), and three OHs (glycerol).

4.2 *FTIR Spectroscopy analysis*

In order to explain the variation of the transport number of lithium, we used infrared spectroscopy to make in evidence the coordination of glycerol by lithium in the concentration range studied. For this purpose, we have made measurements of FTIR of the three concentrations of lithium electroltes 0.056, 0.112, and 0.168 mol. L^{-1} using the spectrophotometer *Perkin Elmer Spectrum 2* to highlight the conformation of the pristine glycerol and electrolytes solutions. To this end, we have evoked the conformation of glycerol, knowing that three structural arrangements α, β and γ of the CH_2OH and OH groups of this molecule are possible; each CH_2OH group in the molecule could revolve around the C-C covalent bond. In this group, the oxygen is in the transposition with respect to the hydrogen of CHOH, which results in the existence of the different conformations, where internal hydrogen bonds are important for their stability. As shown in Figure 2, molecular dynamics studies reveal that the αα, αγ conformations are the most stable and abundant in the liquid phase [36].

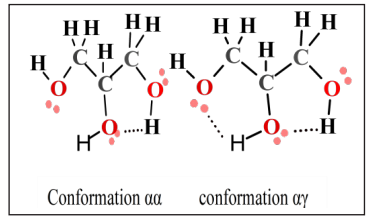

Figure 2: The αα and αγ molecular conformations of glycerol as proposed in the literature.

Table 1: Transference numbers of lithium at infinite dilution in various organic solvents at 298 K

Solvent	Relative Dielectric Constant	Viscosity (10^4 Pa.s)	Number of Hydroxyl Groups	t^0_{Li+}
Water	78.3	8.9	02	0.336 (a)
Ethylene Glycol	40.7	168.4	02	0.294 (b)
Glycerol	42.7	9100	03	0.283 (*)
Ethanol	24.6	10.78	01	0.439 (b)
Methanol	32.7	5.45	01	0.431 (b)

(*) Our work; (a) [35]; (b) [27]

In this context, Pagot *et al.* proposed that the glycerol molecule can exhibit four distinct coordination geometries with lithium [37]. In effect, this metal cation can therefore be coordinated by

- Four glycerol molecules via four monodentate bonds,
- One molecule as a bidentate ligand and two

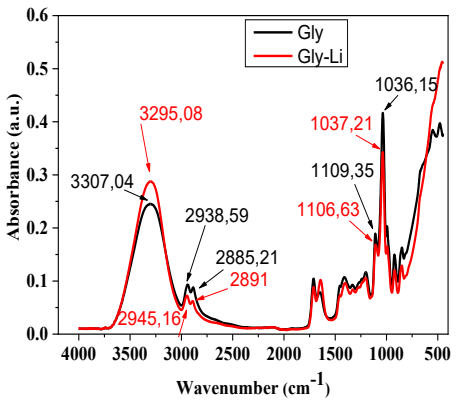

Figure 3: Infrared spectra of the pristine glycerol and the glycerol –lithium solution in the frequency range 800–4000 cm^{-1}.

other molecules as monodentate ligands.

- Two molecules as bidentate ligands.
- One molecule as a monodentate ligand, while another molecule as a tridentate ligand.

4.2.1 Spectrum of a glycerol molecule

As shown in Figure 3, IR spectrum analysis of the glycerol molecule shows a wide and intense band at 3307.04 cm^{-1}, corresponds to the OH group that is involved in the formation of the hydrogen bonds, and two bands located at the wavenumbers 2938.59 cm^{-1} and 2885.21 cm^{-1}, assigned respectively to the CH_2 and CH groups of the backbone of the glycerol molecule. There are bands associated with the C-C-O vibrational extension of alcohol; the first one, acute and intense, located at 1036.15 cm^{-1}, represents the primary alcohol and that of the secondary alcohol located at 1109.35 cm^{-1}. The band located at the wavenumber 994.28 cm^{-1} corresponds to the trans-position [38].

4.2.2 Spectrum of glycerol-lithium complex

Whatever the lithium concentration, the IR spectra reveal the following observations. In effect, after the coordination of the glycerol molecule by the lithium, we notice that the OH elongation vibration and the CO elongation vibrations of primary and secondary alcohols culminating between 1000 and 1100 cm^{-1}, are the most affected by the presence of lithium. Moreover, in order to highlight the differences between the molecule of the solvent (Gly) and the electrolyte (Gly-Li), we have superseded their infrared spectra (Figure 3), where we can observe amply that the OH elongation vibration is shifted to lower wavenumbers with reducing intensity. This behaviour may be explained by the fact that the hydroxyl groups are fully involved in the formation of hydrogen bonds. Indeed, their number reduces considerably when the lithium concentration increases. In addition, the decrease of the OH wavenumber results from the weakening of the strength of the hydrogen-oxygen bond that allows the Li-O bond in glycerol. While, the most affected peaks of the 2nd region by the presence of Li^+, are those centered at 1036.15 and 1109.35 cm^{-1}; they are attributed to the elongation of the primary and secondary alcohol CO respectively. In addition, it can be observed that they shift towards wavenumbers 1037.21 cm^{-1} and 1106.63 cm^{-1}. In consequence, their intensities decrease in Gly-Li.

4.2.3 Areal percentage

With the aim to establish a probable structure of the system composed with the glycerol-lithium electrolyte, we have proceeded to the tabulation of the areas of the most affected centered peaks of the IR spectra within the regions 2500–4000 and 800–1100 cm^{-1} by using three concentrations of lithium: 0.056, 0.112 and 0.168 mol. L^{-1}. This computation has been carried out with the help of the software OriginPro 8.6. The areal percentage of a peak is equal to its area divided by the total area of all peaks present. The values are given in Table 2. In the wavenumber region (2800–4000 cm^{-1}), as shown in Figure 4(a), in increasing the lithium concentration, the percentage areal of the bands located consecutively at 3307 cm^{-1} and 3296 cm^{-1} differ at the most by 4.55%. However, the peak areas centered at 3150 and 3075 cm^{-1} remain almost constant. This explains that hydrogen bonds are more important than interactions between oxygen and coordinating lithium. Figure 4(b) illustrates these observations. This interesting result is in agreement with those already reported in the literature [37]. The coordination geometry remains the same as that of the glycerol molecule in the absence of the ionic metal (Figure 5). Indeed the geometry g1 allows the gathering of the glycerol molecules and the formation of the hydrogen bonds.

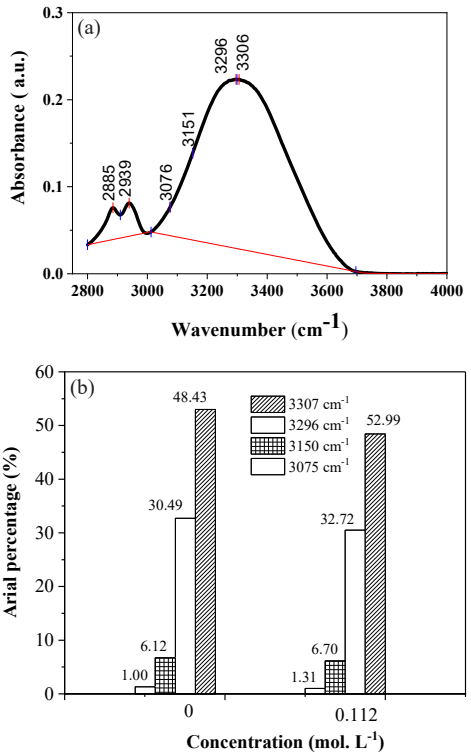

Figure 4: (a) IR spectrum used to compute the areal percentage of the significant peaks for the lithium-glycerol electrolyte (b) Areal percentages (C = 0.112 mol. L^{-1}) in the frequency region 4000–2800 cm^{-1}.

Table 2: Values of the areal percentages (%) of the most affected peaks using the three concentrations

Wavenumber (cm^{-1})	Groupment Assignment	Gly	Gly-Li (a)	Gly-Li (b)	Gly-Li (c)
3307	OH	48.44	49.20	52.99	50.14
3296	OH	30,5	31.68	32.72	29.06
3150	OH	6.12	5.18	6.70	6.07
3075	OH	1.01	1.57	1.32	1.24
2938	CH_2	2.69	2.70	2.75	2.79
2885	CH	2.87	2.61	2.87	2.75
1109	C-C-O (SA)	12.72	12.43	12.13	12.20
1092	C-C-O (SA)	1.56	1.54	1.85	1.52
1075	C-C-O (SA)	3.99	3. 93	3.54	3.86
1058	C-C-O (PA)	8.69	8.54	8.13	8.42
1036	C-C-O (PA)	49.04	48.00	47.89	47.67
994	C-C-O (TP)	13.41	12.90	13.07	12.78

(a) 0.056 mol. L^{-1}; (b) 0.112 mol. L^{-1}; (c) 0.168 mol. L^{-1}

Moreover, as shown in Figure 6(a), in the wavenumber interval 800–1200 cm^{-1}, for the primary alcohol, the vibration band (1036 cm^{-1}) attributed to (C-C-O) is the most affected inducing a difference in the areal percentage of about 1.4%. This indicates that the maximum coordination occurs between the Li^+ cation and the oxygen of the primary alcohol. (Figure 6(b)).

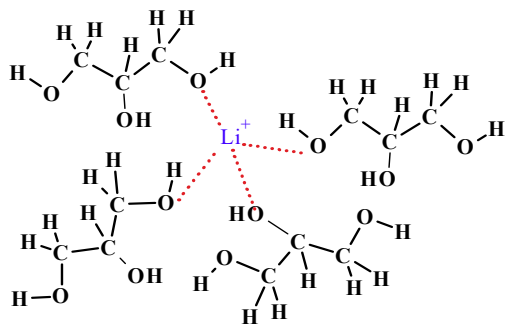

Figure 5: The proposed coordination geometry g_1 of the electrolyte Gly-Li.

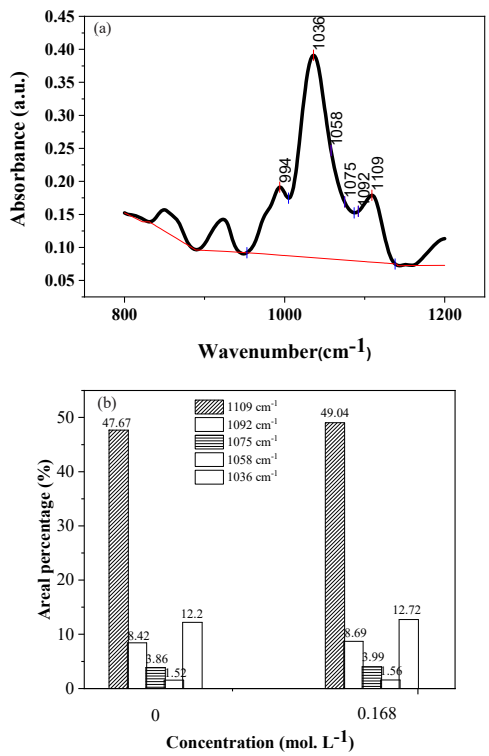

Figure 6: (a) IR spectrum used to compute the areal percentage of the significant peaks for the lithium-glycerol electrolyte (C = 0.168 mol. L^{-1}), (b) Areal percentages in the frequency region 1100–800 cm^{-1}.

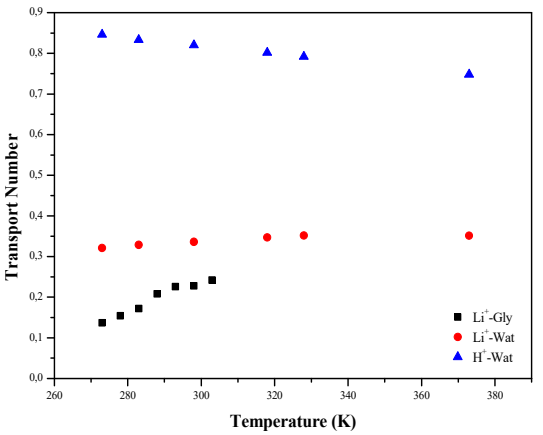

Figure 7: Evolution curve of TN with temperature of CC cell 0.05/0.5: A comparison to aqueous solution data.

4.3 *Effect of temperature*

In the concentration cell with transference, the effect of the temperature is a very important issue to consider. Indeed, when the temperature increases, the voltage rises significantly, as the oxidation/reduction reactions taking place at electrodes are more pronounced. At low temperature, the resistance of the dilute concentration cell (i.e., 0.005/0.05) is too high, and therefore the electromotive force does not vary but fluctuates a little bit. In contrast, beyond the critical temperature (i.e., 283 K), the electromotive force increases drastically and levels out at higher temperatures. While the electromotive force of the most concentrated concentration cell (i.e., 0.5/0.05) increases readily right up from the beginning.

The data of the transport numbers of the lithium ion (t_{Li+}) for the most concentrated cell 0.05/0.5 are illustrated in Figure 7. The transference number increases evidently, as the temperature increases. Thus, it confirmed the greater activation energy of the cation (Li^+) over that of the anion (Cl^-). This finding is similar to that already observed by Munchi *et al.* with the transport numbers of the lithium measured in both the aqueous solution [35] and the polyethylene oxide complexes [39]. The water and glycerol are similar to each other since they have hydroxyl groups, moderate dielectric constants, and can form hydrogen bonds with the nearest neighbors. In effect, since the energy required to separate the cation from the anion is proportional to the ionic radius, considerably less ionic interaction with Cl^- (0.167 nm) than Li^+ (0.090 nm). The same behavior was observed by Munchi *et al.*

Besides, when the concentration gradient rises, the dependence of the transference number upon the temperature declines significantly. It seems reasonable that the transport number of the lithium has the same behavior either in the liquid or solid electrolytes when the temperature changes. Thence, for the concentration cells 0.005/0.05 and 0.5/0.05, the values of the transport numbers were also analyzed and discussed by fitting them to the Arrhenius form of the power law [40].

4.3.1 Fitting data to the power law

The data of the transport number of lithium are essential to determine the performance of high viscous solvents [23] and polymer-based electrolytes [41] in lithium batteries when the temperature varies. For this reason, the experimental data of the transport number (TN) were analyzed versus the temperature, between 0 and 30°C. As suggested in the literature [23], the experimental data were accordingly fitted to the power law given by Equation (7), where the values of the fitting parameters A, B, and the exponent (n) were obtained by carrying out a smooth fitting between the experimental data and the theoretical straight lines, i.e., Ln(TN) versus $(10^3/T)^n$. A least square analysis was then performed, and in consequence, the best values were generally obtained when the value of (n) was close to 2, corresponding to the minimum residual sum of squares. Furthermore, the Arrhenius plots were performed by putting the value of (n) equal to unity. In Figure 8, the straight lines represent the fitted linear equations and their corresponding regression coefficients (R^2). The values of the tabulated fitting parameters are grouped together in Table 3 to highlight how much can the temperature affect the transport properties of the electrolytes

$$\mathrm{Ln(TN)} = A + B\left(\frac{1000}{T}\right)^n \quad (7)$$

Table 3: Values of the fitting parameters of the TN to the power law in the Arrehnius form (n = 1)

Electrolyte	*A*	*B*	*R^2 (%)*
Water-0.05/0.5	2.979	–1.435	95.7
Glycerol-0.05/0.5	4.386	–1.737	95.9
Glycerol-0.005/0.05	48.87	–15.2	92.9

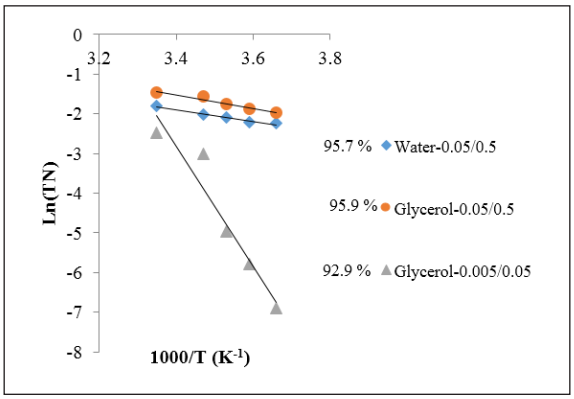

Figure 8: Arrhenius plots of transport number data of concentration cells 0.005/0.05 and 0.05/0.5 using power law in glycerol (Gly.); A comparison to water (Wat.)

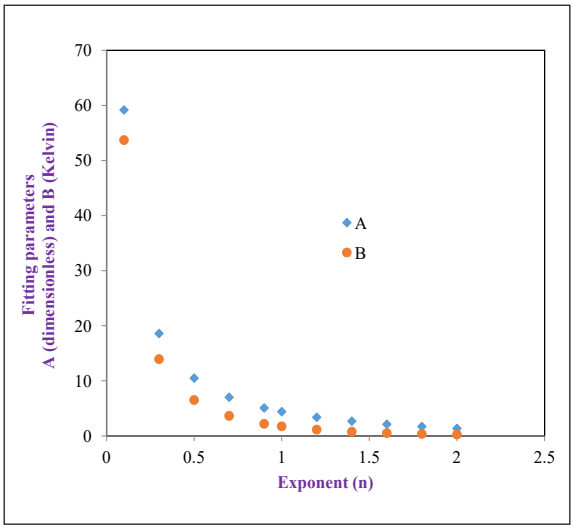

Figure 9: Fitting parameters A (dimensionless) and B (Kelvin) versus exponent (n) assuming the regression coefficient $R^2 \approx 96\%$.

Besides, in order to see the effect of the exponent (n) on the fitting parameters A and B, we have varied its value from 0.1 to 2.0. As shown in Figure 9, both parameters A and B decrease when the value of (n) increases. In effect, there is a steep drop-off in the range (0.1–0.5) upon the modification of the value of (n). However, the values of these two parameters become independent of the change of (n) beyond the Arrhenius type.

4.3.2 Computation of activation energy data

As depicted in Figure 7, the fitting of the transport number to the inverse of the absolute temperature allows the computation of the activation energy (E_a) by using the natural logarithm of the well known Arrhenius relation, i.e., Equation (8) [42] in combination with the power law, i.e., Equation (9) [23]; the parameter (k) being identified as the transport parameter (TN). In effect, when the exponent of the power law (n) is set to unity, the Arrhenius type is obtained i.e., Ln(TN) versus (103/T) in Equation (7), where the slope encloses the values of the gas constant (R) and the activation energy. This latter is readily derived from the fitting parameter B as stipulated in Equation (10).

$$\mathrm{Ln(k)} = \mathrm{Ln(A}_f\mathrm{)} - \frac{E_a}{RT} \tag{8}$$

$$\mathrm{Ln(k)} = A + \frac{1000}{T} B \tag{9}$$

The activation energy E_a can be easily deduced from the slope (i.e., 10^3. B) of the Arrhenius plot of Ln(TN) versus (1/T). Thus,

$$E_a = 10^3 . B . R \tag{10}$$

For glycerol, with the concentration cells 0.005/0.05 and 0.5/0.05, the activation energy values are 31.40 and 22.86 kJ. mol^{-1} respectively, while for water, with concentration cells 0.001/0.01 and 0.5/0.05, the values are 31.73 and 13.59 kJ. mol^{-1} respectively. In effect, at lower concentrations, the activation energy is quite similar between the solvents being hydrogen-bonded and having higher dielectric constants. In contrast, at higher concentrations, the activation energy of glycerol is approximately twice greater than that of water, as the energy required for the coordination between the glycerol molecule and the Lithium is stronger and more sensitive to the solute concentration. Hence, the lifetime of the complex becomes longer. Moreover, according to other investigations [43], [44] the value of the enthalpy of the Li^+/acetonitrile complex formation is estimated to be greater than 12.54 kJ. mol^{-1}).

Moreover, it is observed that in the temperature range 273–303 K and the concentration range 0.005–0.5 mol. L^{-1}, the activation energy may make

in evidence that the overall transport properties, in particular the transference number of the lithium ion, are modulated by the fluctuations of the dipole moments of the glycerol hydroxyl groups. However, as highlighted previously by Pagot *et al*., when the content of Li^+ in the electrolyte is raised, there is no objective correlation between the activation energies of the physical parameters (i.e., the relaxation and the electric conductivity). Indeed, they obtained the activation energy for the relaxation process lower than 23 kJ. mol^{-1} a value which is close to ours, and it was deduced from the analysis of the concentrated concentration cell 0.5/0.05. We may conclude that the migration of the lithium ion is not assisted by the relaxation of the glycerol molecule. However, its overall transport mechanism may be monitored by the diffusion of the conformational states, regardless of the coordination geometry that the glycerol molecule is adopting [38].

5 Conclusions

In the present investigation, the lithium coordination by the viscous hydrogen-bonded glycerol molecule has been shown and estimated. Therefore, it has been computed by calculating the areal percentage of the most affected centered peaks in the FTIR spectrum by using the software OriginPro 8.6. Furthermore, when the concentration increases, its transport number reveals the coordination geometry assumed by the glycerol molecule. Besides, its activation energy can be obtained by means of the Arrhenius analysis. Indeed, for the concentration cell 0.5/0.05, its transport number versus the inverse of the absolute temperature yields activation energy close to that obtained using the conductivity and relaxation parameters. Finally, its overall transport mechanism may be monitored by the diffusion of the conformational states, regardless of the coordination geometry that the glycerol molecule is assuming. This finding has been already highlighted in previous investigations.

Acknowledgements

The authors are indebted to the financial support allocated by the University of Sciences and Technology of Oran (MB). Besides, they are also grateful to Dr. M. A. Benelmouaz for technical assistance during the revision of the paper.

References

[1] M. B. Armand, "Polymer electrolytes," *Annual Review of Materials Science*," vol. 16, pp. 245–261, 1986, doi: 10.1146/annurev.ms.16.080186.001333.

[2] F. M. Gray, *Solid Polymer Electrolytes: Fundamental and Technological Applications*. New York: VCH, 1991.

[3] B. Huang, Z. Pan, X. Su, and L. An, "Recycling of lithium-ion batteries: Recent advances and perspectives," *Journal of Power Sources*, vol. 399, pp. 274–286, 2018, doi : 10.1016/j.jpowsour.2018.07.116.

[4] J. Lopez, M. Gonzalez, J. C. Viera, and C. Blanco, "Fast-charge in lithium-ion batteries for portable applications," presented at NTELEC 2004 the 26th Annual International Telecommunications Energy Conference, Sep. 19–23, 2004.

[5] M. Wakihara, "Recent developments in lithium-ion batteries," in *Materials Science and Engineering*. Florida: CRC Press, 2001, pp. 109–134.

[6] K. D. Fong, J. Self, K. M. Diederichsen, B. M. Wood, B. D. McCloskey, and K. A. Persson, "Ion transport and the true transference number in nonaqueous polyelectrolyte solutions for lithium ion batteries," *American Chemical Society, Central Science*, vol. 5, no. 7, pp. 1250–1260, 2019, doi: 10.1021/acscentsci.9b00406.

[7] G. A. Elia, U. Ulissi, F. Mueller, and J. Reiter, "A long life lithium ion battery with enhanced electrode/electrolyte interface by using an ionic liquid solution," *Chemistry*, vol. 22, no. 20, pp. 6808–6814, 2016, doi: 10.1002/chem.201505192.

[8] L. O. Valøen and J. N. Reimers, "Transport properties of LiPF6-based Li-ion battery electrolytes," *Journal of Tthe Electrochemical Society*, vol. 152, no. 5, pp. 882–891, 2005. doi: 10.1149/1.1872737.

[9] M. Stephan and K. S. Nahm, "Review on composite polymer electrolytes for lithium batterie," *Polymer*, vol. 47, pp. 5952–5964, 2006, doi: 10.1016/j.polymer.2006.05.069.

[10] L. Ye and Z. Feng, "Polymer electrolytes as solid solvents and their applications," *Polymer Electrolytes Fundamentals and Applications*,

pp. 550–582, 2010, doi.org/10.1533/9781845699772.2.550

[11] J. O. Besenhard, M. Winter, J. Yang, and W. Biberacher, "Filming mechanism of lithium-carbon anodes in organic and inorganic electrolytes," *Journal of Power Sources*, vol. 54, pp. 228−231, 1995, doi: 10.1016/0378-7753(94)02073-C.

[12] K. Yuan, H. Bian, Y. Shen, B. Jiang, J. Li, Y. Zhang, H.Chen, and J. Zheng, "Coordination number of Li^+ in nonaqueous electrolyte solutions determined by molecular rotational measurements," *Journal of Physical Chemistry B*, vol. 118, pp. 3689−3695, 2014, doi: 10.1021/jp500877u.

[13] R. J. Blint, "Binding of ether and carbonyl oxygens to lithium ion," *Journal of The Electrochemical Society*, vol. 142, pp. 696−702, 1995, doi: 10.1149/1.2048519.

[14] J. F. Ogara, G. Nazri, and D. M. Macarthur, "A C13 and Li6 nuclear magnetic resonance study of lithium perchlorate poly (ethylene-oxide) electrolytes," *Solid State Ionics*, vol. 47, no. 1–2, pp. 87−96, 1991, doi: 10.1016/0167-2738(91)90185-E.

[15] T. Fukushima, Y. Matsuda, H. Hashimoto, and R. Arakawa, "Solvation of lithium ions in organic electrolytes of primary lithium batteries by electrospray ionization-mass spectroscopy," *Journal of Power Sources*, vol. 110, pp. 34−37, 2002, doi: 10.1016/S0378-7753(02)00168-4.

[16] D. M. Seo, P. D. Boyle, O. Borodin, and W. A. Henderson, "Li^+ cation coordination by acetonitrile-insights from crystallography," *The Royal Society of Chemistry Advances*, vol. 2, pp. 8014−8019, 2012, doi: 10.1039/c2ra21290k.

[17] D. M. Seo, O. Borodin, S. D. Han, P. D. Boyle, and W. A. Henderson, "Electrolyte solvation and ionic association II. Acetonitrile-lithium salt mixtures: Highly dissociated salts," *Journal of The Electrochemical Society*, vol. 159, no. 9, pp. A1489−A1500, 2012, doi: 10.1149/2.035209jes.

[18] S. Seidlmayer, J. Hattendorff, I. Buchberger, L. Karge, H. A. Gasteiger, and R. Gillesa, "In operando small-angle neutron scattering (SANS) on Li-ion batteries," *Journal of The Electrochemical Society*, vol. 162, no. 2, pp. A3116–A3125, 2015, doi: 10.1149/2.0181502jes.

[19] T. K. Zakharchenko, M. V. Avdeev, A. V. Sergeev, A. V. Chertovich, O. I. Ivankov, V. I. Petrenko, Y. Shao-Horn, L. V. Yashina, and D. M. Itkis, "Small-angle neutron scattering studies of pore filling in carbon electrodes: Mechanisms limiting lithium–air battery capacity," *Nanoscale*, vol. 11, pp. 6838–6845, 2019, doi: 10.1039/C9NR00190E.

[20] K. Nishio, "Primary batteries- nonaqueous systems, lithium primary: Overview," *Encyclopedia of Electrochemical Power Sources*, 2009, doi: 10.1016/b978-044452745-5.00115-5.

[21] G. Pagot, S. Tonello, K. Vezzù, and V. D. Noto, "A new glass-forming electrolyte based on lithium glycerolate," *Batteries 4*, vol. 41, no. 3, pp. 1–23, 2018, doi: 10.3390/batteries4030041.

[22] W. Masomboon, T. Sonthisawate, P. Thongjun, and T. R. Srinophakun, "Transesterification of biodiesel by molecular modeling and simulation," *KMUTNB: International Journal of Applied Science and Technology*, vol. 8, no. 1, pp. 45–53, 2015, doi: 10.14416/j.ijast.2014.11.001.

[23] D. C. Champeney and F. O. Kaddour, "Ionic mobility and dielectric relaxation in super-cooled liquid KCl-glycerol solutions," *Molecular Physics*, vol. 52, no. 3, pp. 509–523, 1984, doi:10.1080/00268978400101371.

[24] F. Moulay, M. Mehouen, and M. Kameche, "Transport properties of lithium-ion in green nonaqueous solutions and polymer ionic exchange membranes: An attempt to elaboration of ecological Li- ion battery," *Springer Nature Applied Sciences*, vol. 2, p. 1649, 2020, doi: 10.1007/s42452-020-03449-9.

[25] A. S. Brown and D. A. Macinnes, "The determination of activity coefficients from the potentials of concentration cells with transference I. Sodium chloride at 25°," *Journal of The American Chemistry Society*, vol. 57, no. 7, pp. 1356–1362, 1935, doi: 10.1021/ja01310a055.

[26] D. C. Champeney and H. Comert, "Transference number and activity coefficients of solutions of KCl and NaCl in glycerol using concentration cells," *Physics and Chemistry of Liquids*, vol. 18, no. 1, pp. 43–52, 1988, doi: 10.1080/00319 1088 08078576

[27] M. Spiro, *Physical Chemistry of Organic Solvent Systems*. London, UK: Plenum Press, 1973.

[28] D. C. Champeney and F. O. Kaddour, "Conductance of KCl-glycerol: Test of the Fuoss paired ion model," *Physics and Chemistry of Liquids*, vol. 16,

pp. 239–247, 1987, doi: 10.1080/0031910870 8078526.
[29] P. L. Bailey, *Analysis with Ion-Selective Electrodes*. Kentucky: Hayden, 1980.
[30] R. G. Bates, *Electrometric pH Determinations*. New York: Wiley, 1954.
[31] R. A. Durst, *Ion Selective Electrodes*. Maryland: National Bureau of Standards, 1969.
[32] M. C. Blanco, D. C. Champeney, and M. Kameche, "Transference numbers and activity coefficients of some alkali metal halides in ethylene glycol, using concentration cells," *Physics and Chemistry of Liquids*, vol. 20, no. 2–3, pp. 93–103, 1989, doi: 10.1080/00319108908036396.
[33] D. A. MacInnes and M. Dole, "The transference numbers of potassium chloride. New determinations by the Hittorf method and a comparison with results obtained by the moving boundary method," *Journal of the American Chemical Society*, vol. 53, no. 4, pp. 1357–1364, 1931, doi: 10.1021/ja 01355a025.
[34] K. Izutsu, *Electrochemistry in Nonaqueous Solution*. 2nd ed., Weinheim, Germany: Wiley-VCH, 2009.
[35] A. L. Horvath, *Handbook of Aqueous Electrolyte Solutions: Physical Properties, Estimation and Correlation Methods*. Chichester: Ellis Harwood Chichester, 1985.
[36] C. S. Callam, S. J. Singer, T. L. Lowary, and C. M. Hadad, "Computational analysis of the potential energy surfaces of glycerol in the gas and aqueous phases: Effects of level of theory, basis set, and solvation on strongly intra molecularly hydrogen-bonded systems," *Journal of the American Chemical Society*, vol. 123, pp. 11743–11754, 2001, doi: 10.1021/ja011785r.
[37] G. Pagot, S. Tonello, K. Vezzù, and V. D. Noto, "A new glass-forming electrolyte based on lithium glycerolate," *Batteries 4*, vol. 41, no. 3, pp. 1–23, 2018, doi: 10.3390/batteries4030041.
[38] V. D. Noto, M. Vittadello, S. G. Greenbaum, S. Suarez, K. Kano, and T. Furukawa, "A new class of lithium hybrid gel electrolyte systems," *Journal of Physical Chemistry B*, vol. 108, no. 49, pp. 18832–18844, 2004, doi: 10.1021/jp047413x.
[39] M. Z. A. Munshi, S. Nguyen, and B. B. Owens, "Measurement of Li^+ ion transport numbers in poly(ethyleneoxide)–LiX complexes," *Polymer Journal*, vol. 20, no. 7, pp. 597–602, 1988, doi: 10.1295/polymj.20.597.
[40] A. Hammadi and D. C. Champeney, "Ionic mobility and dielectric relaxation in glass-forming mixtures of sodium chloride and glycerol," *Journal of Solution Chemistry*, vol. 28, no. 1, pp. 21–34, 1999, doi: 10.1023/A:1021747223332.
[41] K. M. Diederichsen, H. G. Buss, and B. D. McCloskey, "The compensation effect in the Vogel–Tammann–Fulcher (VTF) equation for polymer-based electrolytes," *American Chemical Society*, vol. 50, no. 10, 2017, doi: 10.1021/acs. macromol.7b00423.
[42] D. Johns and A. Hutton, "The Arrhenius Law - Arrhenius Plots," 2020. [Online]. Available: https://chem.libretexts.org/@go/page/1447
[43] J. R. Zheng and M. D. Fayer, "Solute- solvent complex kinetics and thermodynamics probed by 2D-IR vibrational echo chemical exchange spectroscopy," *Journal of Physical Chemistry B*, vol. 112, pp. 10221−10227, 2008, doi: 10.1021/ jp804087v.
[44] J. R. Zheng and M. D. Fayer, "Hydrogen bond lifetimes and energetics for solute/solvent complexes studied with 2D-IR vibrational echo spectroscopy," *Journal of The American Chemical Society*, vol. 129, pp. 4328−4335, 2007.